Supplement of Atmos. Chem. Phys., 16, 12397–12410, 2016
http://www.atmos-chem-phys.net/16/12397/2016/
doi:10.5194/acp-16-12397-2016-supplement

Atmospheric Chemistry and Physics Open Access EGU

Supplement of

Mineralogical properties and internal structures of individual fine particles of Saharan dust

Gi Young Jeong et al.

Correspondence to: Gi Young Jeong (jearth@anu.ac.kr)

Supplement Table 1. Ratio of three axes of ellipsoidal dust particles and their iron (hydr)oxide volume %.

Particle No.	Axis			Iron (hydr)oxides
	c	b	a	%
1	1.4	1.0	0.3	1.2
2	1.3	1.0	0.8	0.6
3	1.1	1.0	0.5	50.0
4	1.3	1.0	0.1	0.0
5	1.1	1.0	0.3	0.5
6	1.3	1.0	0.1	3.5
7	1.3	1.0	0.3	1.7
8	2.0	1.0	0.3	5.5
9	1.3	1.0	0.3	0.0
10	1.1	1.0	0.3	2.9
11	1.5	1.0	0.6	9.4
12	1.6	1.0	0.5	55.7
13	1.3	1.0	0.3	0.0
14	1.2	1.0	0.6	91.2
15	1.2	1.0	0.8	5.0
16	1.7	1.0	0.4	0.5
17	1.9	1.0	0.1	3.6
18	2.0	1.0	0.7	0.0
19	1.7	1.0	0.5	2.0
20	1.1	1.0	0.3	8.6
21	1.1	1.0	0.5	3.0
22	1.2	1.0	0.4	1.5
23	1.5	1.0	0.3	0.8
24	1.2	1.0	0.3	6.7
25	1.4	1.0	0.9	0.4
26	1.2	1.0	0.5	0.8
27	1.0	1.0	0.8	7.7
28	1.5	1.0	0.7	0.7
29	1.4	1.0	0.6	1.2
30	1.2	1.0	0.6	0.6
31	1.2	1.0	0.5	0.0
32	2.0	1.0	1.0	0.0
33	1.2	1.0	0.2	9.1
34	1.4	1.0	0.2	1.0
35	1.5	1.0	0.9	1.2
36	1.8	1.0	0.5	2.3
37	1.2	1.0	0.8	0.1
38	1.1	1.0	0.6	10.4
39	1.5	1.0	0.3	10.1
40	1.1	1.0	0.9	2.6
41	1.4	1.0	0.4	0.0
42	1.4	1.0	0.2	3.2
43	1.1	1.0	0.4	15.0
44	1.3	1.0	1.0	1.9
45	1.4	1.0	0.1	27.6
46	1.6	1.0	0.6	4.2
47	1.6	1.0	0.2	0.1
48	1.7	1.0	1.0	0.0
Average	1.4	1.0	0.6	Average 3.5*
Standard deviation	0.3		0.3	Standard deviation 5.1
Median	1.3		0.5	Median 1.5*

*Excluding exceptionally high iron (hydr)oxide contents (particle 3, 12, 14)

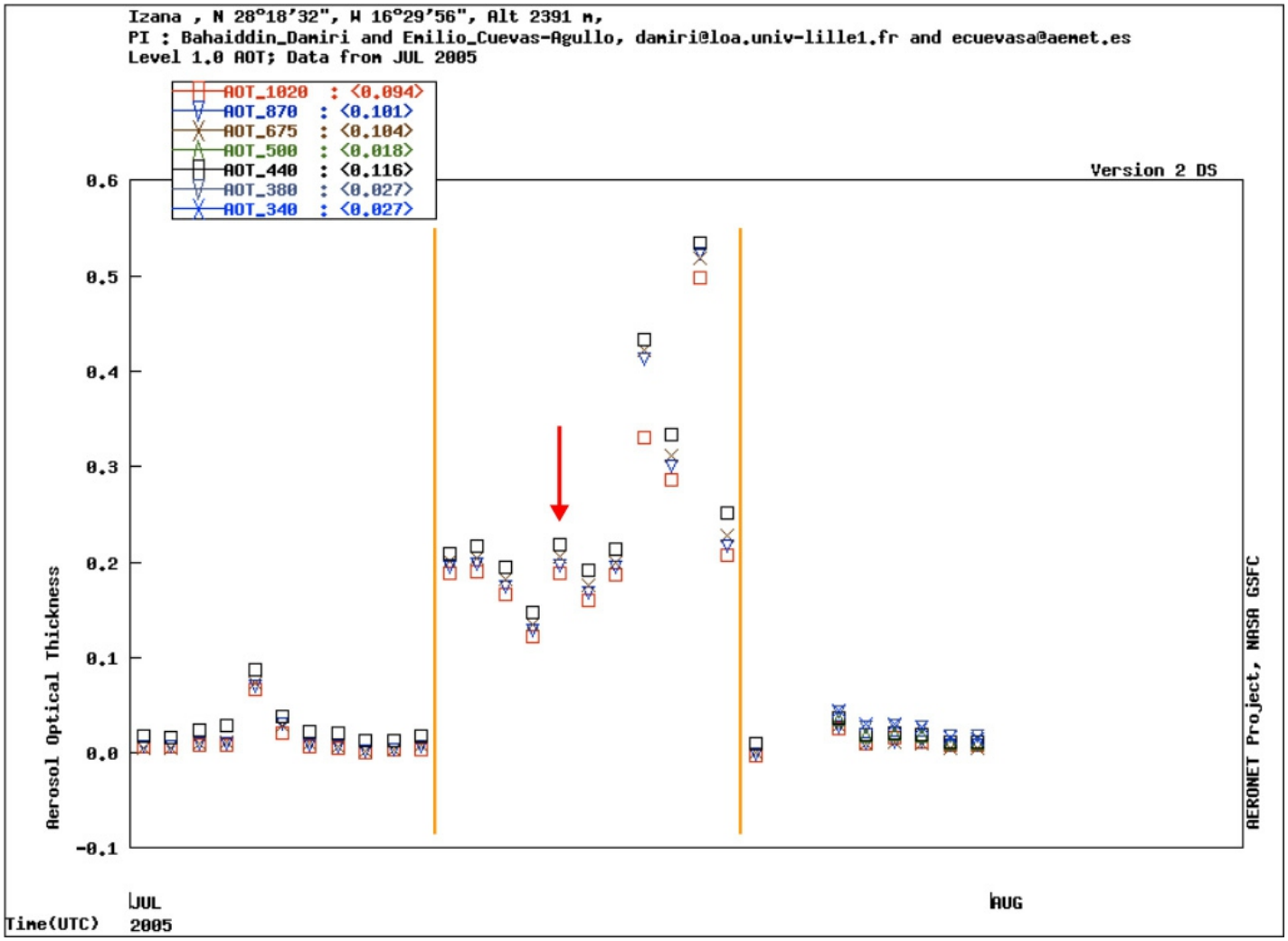

Supplement Fig. 1: Aerosol Robotic Network aerosol optical thickness for Izana, July 2005. Begin and end of the July dust period is marked by orange bars, the sampling day is indicated by a red arrow. Figure created by http://aeronet.gsfc.nasa.gov/cgi-bin/bamgomas_interactive on September 6th, 2016.

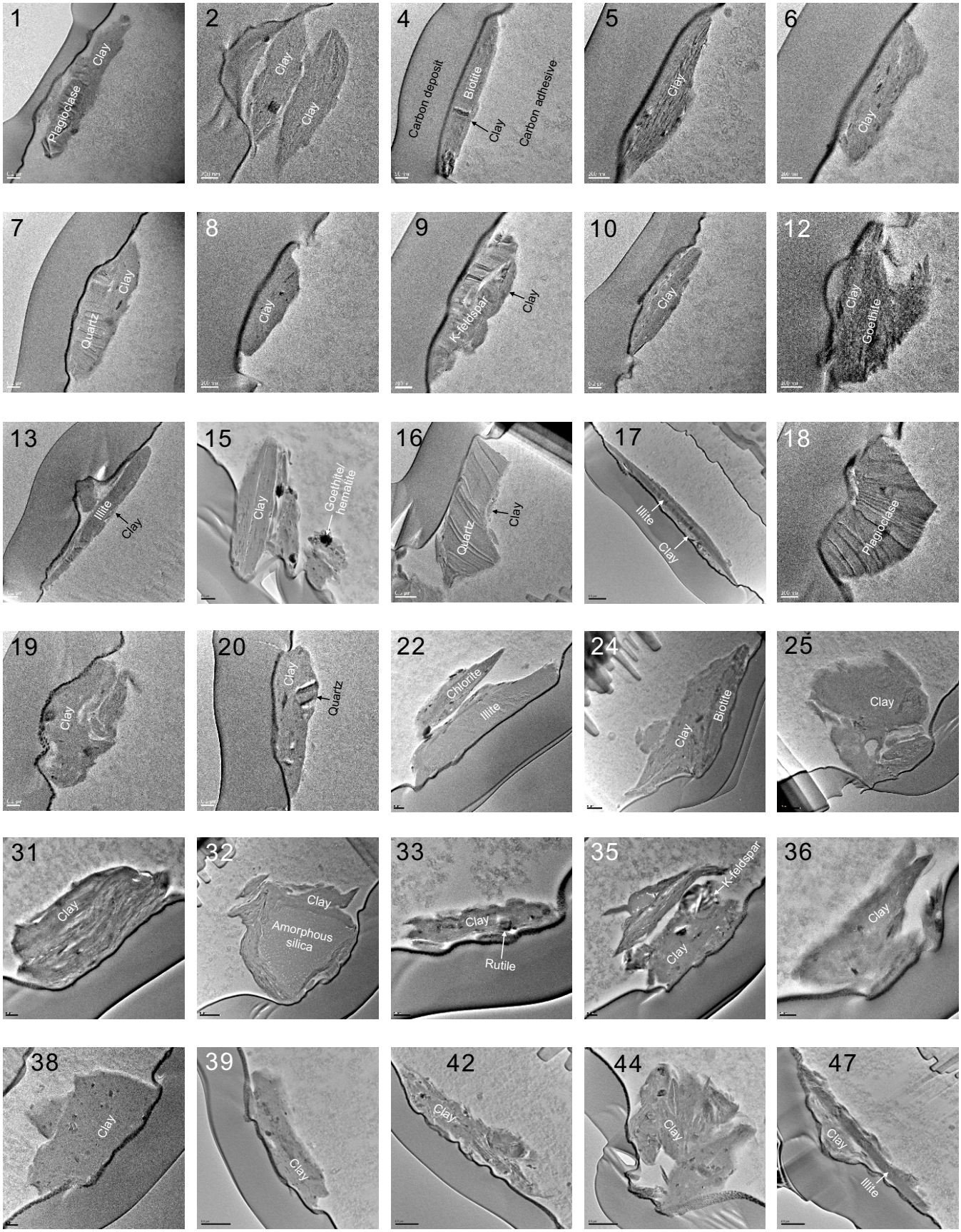

Supplement Fig. 2. TEM images of the cross sections of 30 dust particles not presented in the text.

Supplement Information – Mineral identification

Minerals have their own crystal structures and chemical compositions. Thus, mineral identification using TEM is based on the lattice-fringe imaging and electron diffraction providing structural information and EDXS providing chemical information. Precise identification of all the minerals in the FIB slice to the species level is practically impossible because of beam damage, high vacuum, lower reliability of lattice fringes/electron diffraction data in comparison with XRD, and enormous time required.

TEM identification of nonphyllosilicate minerals

The identification of quartz, K-feldspar, plagioclase, calcite, amphibole, dolomite, titanite, apatite, and gypsum was straightforward based on their characteristic EDX spectra (Fig. S1). Although we could not identify mineral species of K-feldspar (sanidine, orthoclase, microcline), plagioclase (albite, oligoclase, andesine...), and amphibole (tremolite, actinolite, hornblende...) using time-consuming complex operation, the purpose of current mineral dust research was satisfied by grouping similar mineral species. Silica phase of the mineral dust from desert was almost quartz, consistent with XRD although few amorphous silica was identified by electron diffraction.

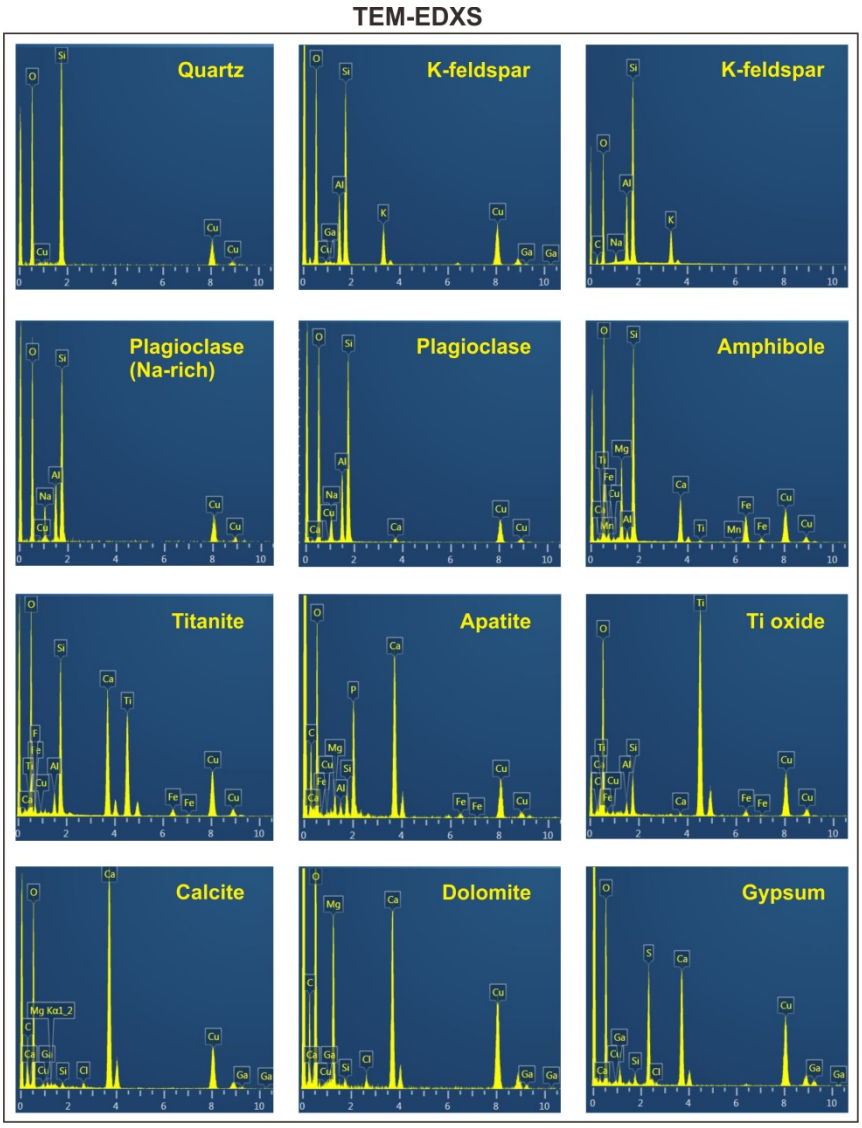

Fig. S1. TEM EDXS patterns of constituent minerals of dust particles obtained from the cross-sectional slices prepared by FIB.

TEM identification of phyllosilicate minerals

Phyllosilicate minerals were abundant in the mineral dust. The identification of muscovite, biotite, and chlorite was rather straightforward from their characteristic chemical compositions with the aid of lattice-fringe imaging (Fig. S2). However, the identification of nano-thin phyllosilicates (clay minerals) was difficult because of their breakdown under electron beam and small grain size below the minimum diameter of electron beam for EDXS. They occurred often as agglomerates. In addition, mixed layering of illite and smectite is common in natural soils. The identification of clay minerals was based on lattice fringes and chemical compositions: 1.0 nm for illite, ~1.0 nm for smectite and vermiculite, and ~7.0 nm for kaolinite (Fig. S2). Kaolinite was directly identified from its EDXS with the aid of lattice fringe imaging. However, illite, smectite, and illite-smectite mixed layers could not be separately identified each other because smectite was contracted under the high vacuum of the TEM chamber, showing ~1.0 nm lattice fringes similar to those of illite. Although EDXS can be used for identifying illite and smectite with interlayer cations K and Ca, respectively, they cannot be separately analyzed using EDXS, even when using an electron beam as small as possible. Therefore, we could not distinguish between nano-thin illite, smectite, and their mixed-layers, using conventional TEM work. To avoid over-interpretation, nano-thin platelets of clay minerals showing ~1.0 nm lattice fringes with varying K and Ca contents were grouped into illite-smectite series clay minerals (ISCMs). ISCMs are nano-scale mixtures of nano-thin platelets of illite, smectite, and illite-smectite mixed-layers.

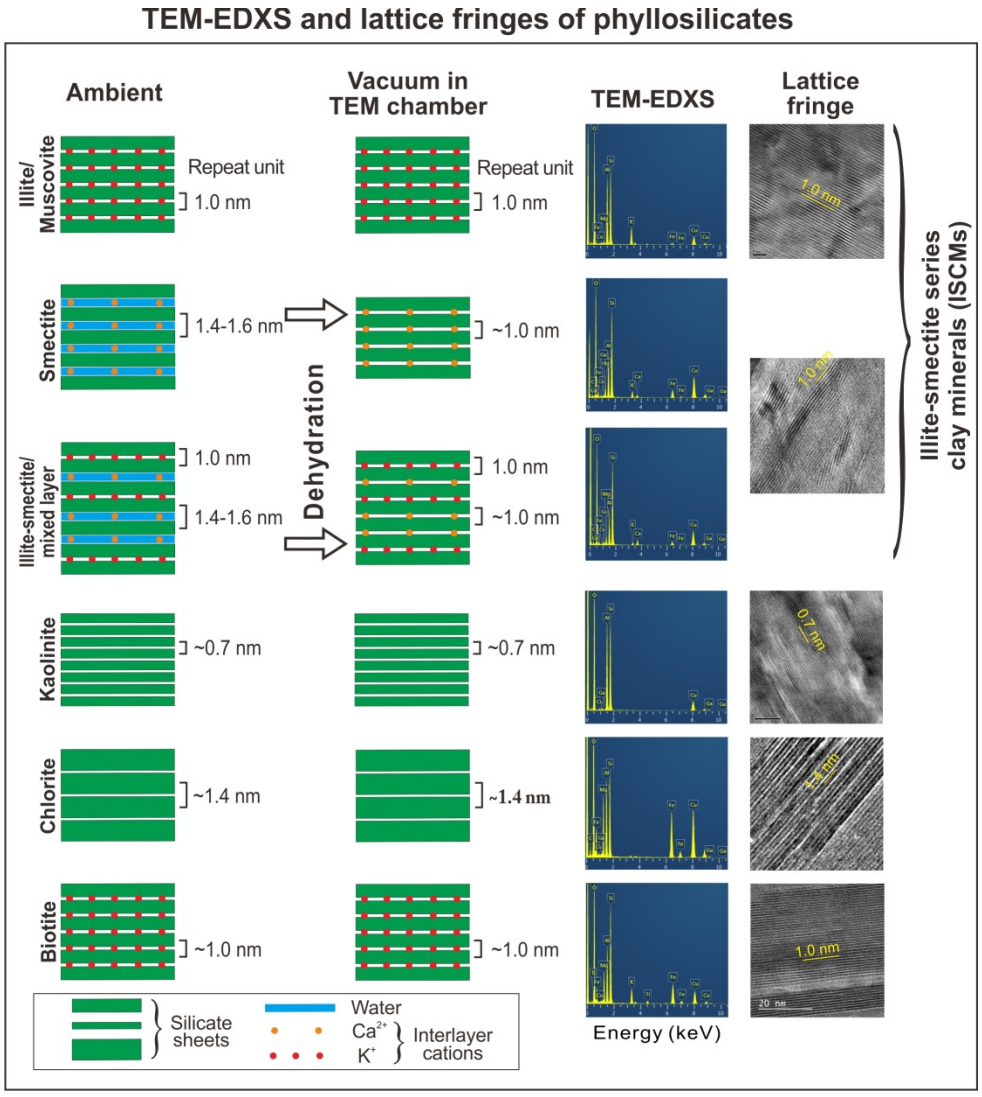

Fig. S2. Identification of phyllosilicates using TEM-EDXS and lattice fringes.

TEM identification of iron (hydr)oxides

Mineralogical identification of iron (hydr)oxides was also challenging. EDXS could not be used for the identification. Electron diffraction and lattice-fringe imaging should be used in combination as shown in Fig. S3. However, many iron (hydr)oxide grains could not be identified because of the overlap of many *d*-spacings, varying crystallographic orientation, and tiny grain sizes. Thus, we used species names only in cases in which mineral species were identified unambiguously by lattice fringe imaging and electron diffraction; in other cases, we used the collective term "iron (hydr)oxide".

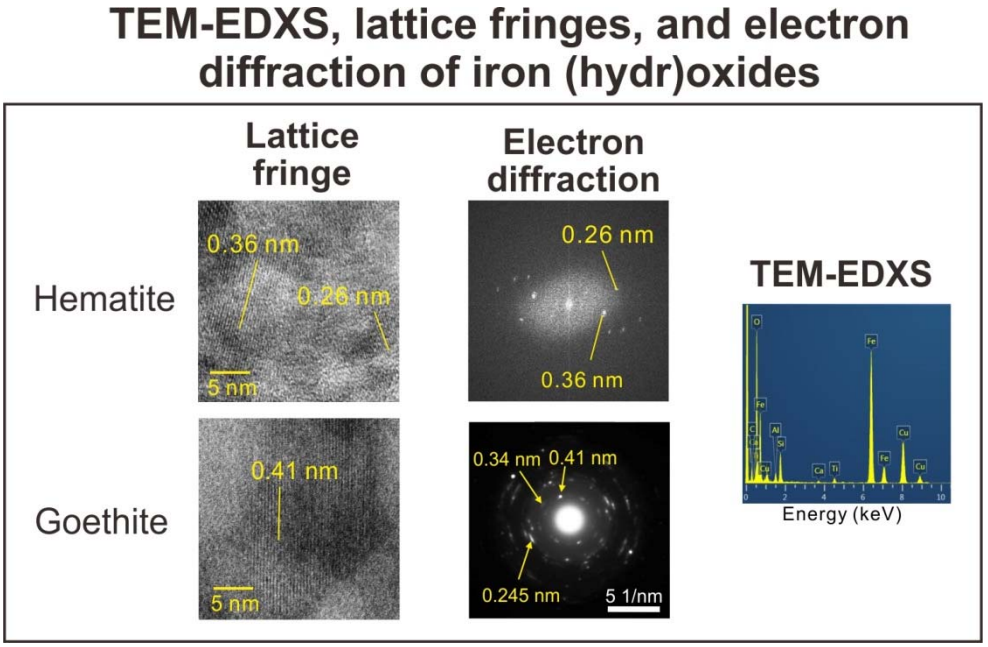

Fig. S3. Identification of phyllosilicates using lattice fringes and electron diffraction.

Mineralogical classification of dust particles using SEM-EDXS

Dust particles are essentially mixtures of mineral grains of diverse species and sizes. In case the quantity of powder dust samples is sufficient (~several hundred mg), XRD method is best for the determination of mineral composition. SEM-EDXS analyses of individual particle can be used when powder samples are insufficient or non-available. Ideally, mineral composition of individual dust particle can be determined by mixing several minerals to get the overall chemical composition of the particle. Then, the summation of the mineral compositions of thousands of dust particles considering their volume would lead to the mineral composition of bulk dust. However, the irregular morphology of dust particles prohibits the accurate determination of dust particles due to the difficulty of calibration. In addition, the chemical compositions of constituent minerals are varied. Prior to the development of reliable quantitative analysis procedure based on SEM for the mineral composition of individual dust particle, we adopted semi-quantitative approach. Since dust particles are generally dominated by one mineral species or group, we have determined the predominant mineral of a dust particle referring to the EDXS patterns of pure minerals as shown in Figs. S1 and S2. In case particles show intermediate EDXS pattern (Fig. S4), half of the particle was counted (0.5). Summation of the counts led to the approximate mineral composition of bulk dust. Although the procedure is evidently semi-quantitative, SEM-EDXS results were consistent with XRD results in the recent analyses of Asian dust (Table 1 in Park and Jeong (2016), Journal of the Mineralogical Society of Korea, 29, 79–87).

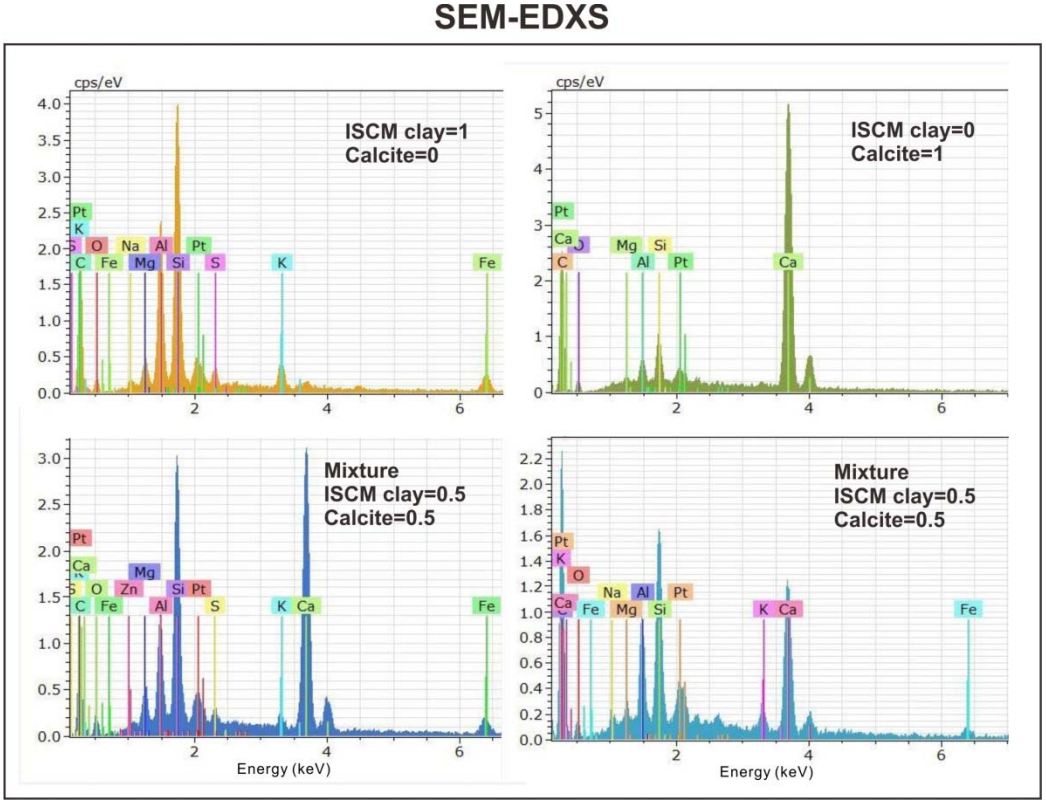

Fig. S4. SEM-EDXS of dust particles.

Park and Jeong (2016)

Table 1. Mineral compositions of Asian dusts determined by XRD analysis and SEM-EDS single particle analysis

Minerals	Asian dust XRD				
	Feb 22 2015	Mar 18 2014	Mar 31 2012	Mar 20 2010	Average
	(This study)	(Jeong and Achterberg, 2014)			
ISCMs	55	60	42	50	51
Kaolinite	2	1	3	4	3
Chlorite	5	3	6	7	5
Total clay	*62*	*64*	*52*	*61*	59
Quartz	18	14	23	15	17
Plagioclase	10	11	15	10	12
K-feldspar	4	0	6	2	3
Amphibole	0	0	1	2	1
Calcite	5	5	2	5	4
Gypsum	1	6	2	6	4
Total	100	100	100	100	100
	SEM single particle analysis				
ISCMs	57	54	48	54	52
Kaolinite	2	1	3	2	2
Chlorite	3	2	4	6	4
Total clay	*62*	*58*	*55*	*62*	58
Quartz	19	19	21	17	19
Plagioclase	9	11	11	10	11
K-feldspar	3	4	5	3	4
Amphibole	0	1	1	0	1
Calcite	4	7	7	6	7
Gypsum	2	0	1	1	1
Total	100	100	100	100	100